Luminescent Properties and Concentration Quenching of Eu²⁺ in Ba₂Ca(BO₃)₂

WANG Zhi-jun[1], LIU Chong[2], YANG Zhi-ping[1]*,

LI Pan-lai[1], GUO Qing-lin[1]

(1. *College of Physics Science & Technology, Hebei University, Baoding 071002, China*;

2. *College of Graduate Studies, Hebei University, Baoding 071002, China*)

* *Corresponding Author*, E-mail：*lipanlai_780616@ yahoo. com. cn*

Abstract：Ba₂Ca(BO₃)₂：Eu²⁺ phosphor was synthesized by a high temperature solid-state method. CaCO₃(A. R), BaCO₃(A. R), H₃BO₃(A. R) and Eu₂O₃(99.99%) were used as raw materials. Its crystal structure, luminescent characteristics and Commission International de l'Eclairage (CIE) chromaticity coordinates values were measured. Under the ultraviolet to visible light irradiation, Ba₂Ca(BO₃)₂：Eu²⁺ shows an asymmetrically single green emission band with a maximum at 537 nm, which corresponds to the 4f⁶5d¹→4f⁷ transition of Eu²⁺. The emission intensity of Ba₂Ca(BO₃)₂：Eu²⁺ was influenced by Eu²⁺ molefraction, at first, it increases with the increase of Eu²⁺ mole fraction, and reaches a maximum value at 2% Eu²⁺, then decreases with further increasing its concentration because of the concentration quenching effect. And the concentration quenching mechanism is verified to be dipole-dipole interaction. According to the crystal structure data and the experimental spectral data, the critical distances(R_c) can be obtained, and are 2.64 nm and 2.11 nm, respectively. Moreover, with increasing the Eu²⁺ doped content, the CIE chromaticity coordinates of the samples were slightly varied. For Ba₂Ca(BO₃)₂：2% Eu²⁺, the quantum efficiency is approximately 72%.

Key words：luminescence；Eu²⁺；Ba₂Ca(BO₃)₂；concentration quenching

CLC number：TN383⁺.1　　**Document code**：A　　**DOI**：10.3788/fgxb20123307.0729

Eu²⁺ 在 Ba₂Ca(BO₃)₂ 中的发光特性及浓度猝灭

王志军[1]，刘　冲[2]，杨志平[1]*，李盼来[1]，郭庆林[1]

(1. 河北大学 物理科学与技术学院，河北 保定　071002；

2. 河北大学 研究生学院，河北 保定　071002)

摘要：采用高温固相法，以 CaCO₃(A. R)、BaCO₃(A. R)、H₃BO₃(A. R) 和 Eu₂O₃(99.99%) 为原料制备了 Ba₂Ca(BO₃)₂：Eu²⁺ 绿色发光材料，测量了材料的晶体结构、发光特性及色坐标等。Ba₂Ca(BO₃)₂：Eu²⁺ 材料的激发光谱覆盖 200～500 nm 的紫外-可见光区。在 400 nm 近紫外光激发下，材料的发射光谱为一主峰位于 537 nm 的非对称宽谱，对应于 Eu²⁺ 的 4f⁶5d¹→4f⁷ 特征跃迁。研究发现，随 Eu²⁺ 掺杂浓度的增大，Ba₂Ca-(BO₃)₂：Eu²⁺ 材料的发射强度呈现先增大、后减小的变化趋势，最大发射强度对应的 Eu²⁺ 掺杂摩尔分数为

2%。造成发射强度下降的原因为浓度猝灭,其机理为电偶极-电偶极相互作用。依据晶格常数及实验光谱数据,得出临界距离 R_c 分别为 2.64 nm 和 2.11 nm。随 Eu^{2+} 掺杂浓度的增大,$Ba_2Ca(BO_3)_2$:Eu^{2+} 材料的色坐标变化微小。计算得到 $Ba_2Ca(BO_3)_2$:2% Eu^{2+} 的转换效率约为 72%。

关 键 词:发光;Eu^{2+};$Ba_2Ca(BO_3)_2$;浓度猝灭

1 Introduction

A large number of borate compounds have a wide emission distributing under the ultraviolet (UV) to visible light irradiation, therefore, they are regarded as a kind of promising optoelectronic materials[1-11]. Recently, some researches focus on the materials, for example, Verstegen reported the luminescent properties of Tb^{3+} in $X_2Z(BO_3)_2$ (X = Ba, Sr; Z = Ca, Mg)[12]; Keszler *et al.* investigated the luminescent properties of $X_2Z(BO_3)$ (X = Ba, Sr; Z = Ca, Mg): Eu^{2+} [13-15]; Liu *et al.* depicted the luminescent properties of Tb^{3+}, Tm^{3+} or Dy^{3+} doped $Ba_2Ca(BO_3)_2$ or $Sr_2Mg(BO_3)_2$ [16-17]; Lin *et al.* synthesized Ce^{3+} or Eu^{2+} doped $Ba_2Mg(BO_3)_2$ or $Ba_2Ca(BO_3)$ phosphors, and studied its luminescent properties[18-19]. In order to further study the luminescent properties of rare earths in the alkaline earth orthoborate, the Eu^{2+} doped $Ba_2Ca(BO_3)_2$ phosphor was synthesized in our previous work[20]. In this research, in attempts to contribute to the further research on $Ba_2Ca(BO_3)_2$:Eu^{2+} phosphor, the luminescent properties and concentration quenching of Eu^{2+} in $Ba_2Ca(BO_3)_2$ were studied.

2 Experiments

A series of $Ba_2Ca(BO_3)_2$:x% Eu^{2+} (mole fraction) were synthesized by the high temperature solid-state reaction method. $CaCO_3$(A.R), $BaCO_3$ (A.R), H_3BO_3(A.R) and Eu_2O_3(99.99%) were used as raw materials, which were stoichiometrically weighed and thoroughly mixed in an agate mortar. The mixed powders were calcined in corundum crucibles, then, were introduced into a muffle furnace sintered at 1 000 ℃ for 5 h in a reducing atmosphere (a mixture of H_2(5%) and N_2(95%). Finally the samples were cooled down to room temperature and ground thoroughly again into powders. Moreover, all the phosphors are washed and sieved under the same condition to ensure the similar particle size distribution.

The crystal structure of the synthesized powders was characterized by X-ray powder diffraction using D/max-rA X-ray diffractometer with Cu Kα radiation (λ = 0.154 06 nm) operated at 40 kV and 100 mA. The spectral characteristics were performed by using a Shimadzu RF-540 fluorescence spectrophotometer equipped with a xenon discharge lamp as an excitation source. The Commission International de l'Eclairage (CIE) chromaticity coordinates values were measured by using a PMS-80 UV-VIS-NEAR IR Spectrorphotocolorimeter. All the properties of the phosphors were measured at room temperature.

3 Results and Discussion

3.1 Crystal Structure

XRD patterns of $Ba_2Ca(BO_3)_2$:x% Eu^{2+} (x = 0.5, 1, 2, 3, 5, 7) phosphors were measured, and the all XRD patterns agreed well with the standard
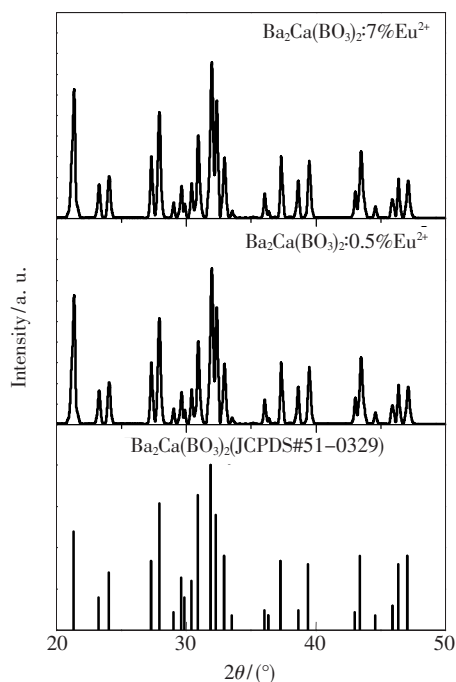

Fig. 1 XRD patterns of $Ba_2Ca(BO_3)_2$:x% Eu^{2+} (x = 0.5, 7) phosphors with the standard data of $Ba_2Ca(BO_3)_2$

data of $Ba_2Ca(BO_3)_2$ phase (JCPDS #51-0329), which means that the doped Eu^{2+} do not change general structure. As a representative, Fig. 1 shows the XRD patterns of $Ba_2Ca(BO_3)_2$: $x\% Eu^{2+}$ (x = 0.5,7) phosphors. $Ba_2Ca(BO_3)_2$ has a monoclinic crystal structure, and its lattice parameters values are a = 1.422 0 nm, b = 0.457 0 nm, c = 1.193 0 nm.

In order to further confirm the occupation site of Eu^{2+} in the host lattice. The crystal unit cell parameters were calculated by using the XRD data with Jade 5.0 software, and the lattice parameters of $Ba_2Ca(BO_3)_2$: $x\% Eu^{2+}$ (x = 0.5,1,2,3,5,7) phosphors were listed in Table 1. It shows that a, b, and c are a little smaller than the standard data (JCPDS No. 51-0329). The results of Ref [18-20] indicate, for $Ba_2Ca(BO_3)_2$, Eu^{2+} and Ce^{3+} always preferentially replace Ba^{2+} sites at low doping concentration. Therefore, the decrease of the crystal unit cell parameters is due to the smaller radii of incorporated Eu^{2+} (0.130 nm) than that of Ba^{2+} (0.147 nm)[5].
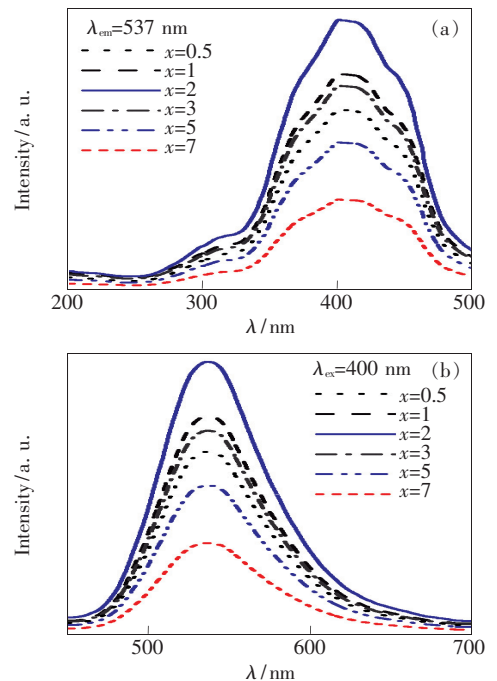
Table 1   The structure parameters of $Ba_2Ca(BO_3)_2$: $x\% Eu^{2+}$

Samples	a/nm	b/nm	c/nm	V/nm³
$Ba_2Ca(BO_3)_2$ (JCPDS#51-0329)	1.422 0	0.457 0	1.193 0	0.775 3
$Ba_2Ca(BO_3)_2$: 0.5% Eu^{2+}	1.421 7	0.456 6	1.192 7	0.774 2
$Ba_2Ca(BO_3)_2$: 1% Eu^{2+}	1.421 1	0.456 1	1.192 2	0.772 7
$Ba_2Ca(BO_3)_2$: 2% Eu^{2+}	1.420 6	0.455 7	1.191 6	0.771 4
$Ba_2Ca(BO_3)_2$: 3% Eu^{2+}	1.420 2	0.455 2	1.191 3	0.770 1
$Ba_2Ca(BO_3)_2$: 5% Eu^{2+}	1.411 8	0.454 6	1.190 8	0.764 3
$Ba_2Ca(BO_3)_2$: 7% Eu^{2+}	1.411 3	0.454 2	1.190 3	0.763 0

3.2   Luminescent Properties of $Ba_2Ca(BO_3)_2$: Eu^{2+} Phosphor

Fig. 2 depicts the emission and excitation spectra of $Ba_2Ca(BO_3)_2$: $x\% Eu^{2+}$ (x = 0.5,1,2,3,5, 7). The results show that the positions of excitation and emission bands have no obvious change for all the phosphors. They exhibit green emission band centred at 537 nm, which corresponds to the f-d transition of Eu^{2+}. The broad luminescence of Eu^{2+} is due to the $4f^6 5d^1 \rightarrow 4f^7$ transition, which is an allowed electrostatic dipole transition. However, the 5d state is easily affected by the crystal field, that is to say, different crystal fields can split the 5d state in different ways[18-20], and Eu^{2+} ions can replace Ba^{2+} and Ca^{2+} sites in $Ba_2Ca(BO_3)_2$. It can be seen from Fig. 2, at frist, the emission intensity of Eu^{2+} increases with increase of its concentration, and reaches the maximum at 2% Eu^{2+}, then decreases with further increasing its concentration because of the concentration quenching effect.

In our previous work[20], the concentration quenching mechanism is cursorily explored, and is dipole-dipole interaction by Dexter theory. However,

Fig. 2   (a) Excitation and (b) emission spectra of $Ba_2Ca(BO_3)_2$: $x\% Eu^{2+}$ (x = 0.5,1,2,3,5,7) phosphors.

if using the Dexter theory, some conditions must be considered, so the concentration quenching mechanism of Eu^{2+} in $Ba_2Ca(BO_3)_2$ ought to be anew discussed. According to Blasse[21], if the activator is

introduced solely on Z (for $Ba_2Ca(BO_3)_2$, $Z = Ba$, Ca) ion sites, x_c is the critical concentration. N is the number of Z ions in the unit cell and V is the volume of the unit cell, the critical distance (R_c) of energy transfer can be calculated by using the concentration quenching method, and estimated by the following formula[21]

$$R_c \approx 2 \left[3V/(4\ x_c N) \right]^{1/3}. \quad (1)$$

However, $Ba_2Ca(BO_3)_2 : Eu^{2+}$ has an asymmetrically emission band which means two Eu^{2+} sites in $Ba_2Ca(BO_3)_2$. $Ba_2Ca(BO_3)_2$ belong to the monoclinic system with space group $C2/m$. There is only one Ba site which is asymmetrically coordinated by nine oxygen atoms in the Cs symmetry. The Ca atom occupies a slightly distorted octahedral site. When Eu^{2+} ion is incorporated in $Ba_2Ca(BO_3)_2$, it may substitute for Ba^{2+} or Ca^{2+}. When Eu^{2+} replaces one specific type of alkaline earth sites (either Ba^{2+} or Ca^{2+}), the doped compound will show only one center emission. However, a dissymmetrical emission band was observed, it indicates that the emission from two different luminescent centers. Because the ionic radius of Eu^{2+} is smller than that of Ba^{2+}, but it is bigger than that of Ca^{2+}. For $Ba_2Ca(BO_3)_2 : Eu^{2+}$, two different luminescent centers are associated with Eu^{2+} on both the Ba^{2+} and Ca^{2+} sites. The stronger band of Eu^{2+} which originated from the Eu^{2+} replace Ba^{2+} sites, while weak band is due to the emission of Eu^{2+} in Ca^{2+} sites[20].

Under the 400 nm light irradiation, the spectral properties of $Ba_2Ca(BO_3)_2 : x\% Eu^{2+}$ ($x = 0.5, 1, 2, 3, 5, 7$) were studied, and the fit bands which correspond to the two Eu^{2+} centers in $Ba_2Ca(BO_3)_2$ are shown in Fig. 3. The two fit bands are located at 531 and 568 nm, respectively. Fig. 3 presents that the intensity of the two fit bands, at first, increases with increase of Eu^{2+} concentration, reaches a maximum value at 2% Eu^{2+}, then decreases with further increasing its concentration. It means that the two emission centers have the same concentration quenching process. Though Eu^{2+} replaced the Ba^{2+} and Ca^{2+} sites, however, the emission which orginates from Eu^{2+} substituting for Ba^{2+} sites is always dominant. Moreover, the two Eu^{2+} emission centers

have the same critical concentration. Therefore, the concentration quenching mechanism of Eu^{2+} in $Ba_2Ca(BO_3)_2$ can be approximately calculated by Blasse' formula (1). By taking the appropriate values of V, N and x_c (0.771 4 nm^3, 4, 2%, respectively), the critical distance (R_c) of Eu^{2+} in $Ba_2Ca(BO_3)_2$ is found to be 2.64 nm.
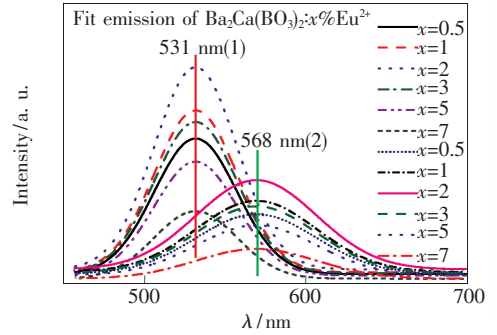

Fig. 3　Fit emission spectra of $Ba_2Ca(BO_3)_2 : x\% Eu^{2+}$ ($x = 0.5, 1, 2, 3, 5, 7$) phosphors. Band 1 located at 531 nm, and band 2 located at 568 nm.

According to Dexter's theory on non-radiative energy transfer, the critical distance (R_c) of Eu^{2+} can also be calculated from the spectral experimental data, and be found from[22]

$$R_c^6 = 0.63 \times 10^{28}(4.8 \times 10^{-16} P/E^4)SO, \quad (2)$$

where P is the oscillator strength of the absorption transition of Eu^{2+} ion, E the energy of maximum spectral overlap, and SO the spectral overlap integral. For P a value of 0.01 for the broad $4f^7 \rightarrow 4f^6 5d^1$ absorption band is taken. E and SO, which are derived from the spectral experimental data, are 2.03 eV and 0.05 eV^{-1}, respectively. Therefore, a values of $R_c = 2.11$ nm is obtained. Thus, it based on the calculated crystal structure data is in agreement with that of the experimental spectral data.

3.3　Concentration Quenching Mechanism of Eu^{2+} in $Ba_2Ca(BO_3)_2 : Eu^{2+}$ Phosphor

Non-radiative energy transfer from one Eu^{2+} ion to another Eu^{2+} ion may occur by exchange interaction, radiation reabsorption or multiple-multiple interaction. Eu^{2+} is an isolated emission center in $Ba_2Ca(BO_3)_2 : Eu^{2+}$ phosphors. The $4f^7 \rightarrow 4f^6 5d^1$ transition of Eu^{2+} is allowed while exchange interaction is responsible for the energy for forbidden transitions and typical critical distances are then about

0.5 nm[22]. It means that the mechanism of exchange interaction plays no role in energy between Eu^{2+} ions in $Ba_2Ca(BO_3)_2$：Eu^{2+} phosphor. The mechanism of radiation reabsorption comes into effect only when there is broad overlap of the fluoresent spectra of the sensitizer and activator and in the view of the emission and excitation spectra of $Ba_2Ca(BO_3)_2$：Eu^{2+} phosphor is unlikely to be occuring in the case. The concentration quenching mechanism of Eu^{2+} in $Ba_2Ca(BO_3)_2$：Eu^{2+} ought to be the electric multiple-multiple interaction by using Dexter's theory. If the energy transfer occurs between the same sorts of activators, the multipolar interaction can be determined from the change of the emission intensity. The emission intensity per activator ion follows the equation[23-24]

$$I/x = K[1 + \beta(x)^{Q/3}]^{-1}, \qquad (3)$$

where x is the activator concentration; $Q = 6,8,10$ for dipole-dipole (d-d), dipole-quadrupole (d-p), quadrupole-quadrupole (q-q) interactions, respectively; K and are constant for the same excitation conditions for a given host crystal.

The inset of Fig. 4 shows the emission intensity of Eu^{2+} in $Ba_2Ca(BO_3)_2$ under the 400 nm light irradiation, and it reaches the maximum value at $2\% Eu^{2+}$. Fig. 4 presents the plot of $lg(I/x)$ as a function of lgx in $Ba_2Ca(BO_3)_2$：Eu^{2+}. The dependence of $lg(I/x)$ on lgx is linear and the slope is

-1.85. Therefore, the value of Q can be calculated as 5.55, and approximately equal to 6. It means that the concentration quenching mechanism of Eu^{2+} in $Ba_2Ca(BO_3)_2$ is the d-d interaction.

Fig. 4   Plot of $lg(I/x)$ as function of lgx in $Ba_2Ca(BO_3)_2$： $x\% Eu^{2+}$ ($x = 0.5,1,2,3,5,7$) phosphors ($\lambda_{ex} = 400$ nm). The inset：the emission intensity of $Ba_2Ca(BO_3)_2$：$x\% Eu^{2+}$ phosphors as function of Eu^{2+} concentration ($x = 0.5, 1,2,3,5,7$).

3.4   Chromaticity Coordinates and Quantum Efficiency of $Ba_2Ca(BO_3)_2$：Eu^{2+}

Under 400 nm excitation, the CIE chromaticity coordinates of $Ba_2Ca(BO_3)_2$：$x\% Eu^{2+}$ ($x = 0.5,1, 2,3,5,7$) were measured, and shown in Table 2. With increasing the Eu^{2+} concentration, the CIE chromaticity coordinates slightly varied. And the little change in positions from $x = 0.5$ to $x = 7$ could be due to change in the crystal field surrounding the activator cations of Eu^{2+} [25].

Table 2   The CIE chromaticity coordinates of $Ba_2Ca(BO_3)_2$：$x\% Eu^{2+}$

Samples	$x = 0.5$	$x = 1$	$x = 2$	$x = 3$	$x = 5$	$x = 7$
CIE (x, y)	0.188, 0.627	0.189, 0.627	0.190, 0.627	0.191, 0.627	0.191, 0.628	0.191, 0.628

For photoluminescent applications, the quantum efficiency of phosphor is often regarded as a measure of its figure of merit. Quantum efficiency of the $Ba_2Ca(BO_3)_2$：$2\% Eu^{2+}$ is calculated by the method described by De Mello and Pålsson[26-27]. Briefly, the method allows determining the sample quantum efficiency ϕ_f by measuring the ration between the number of photons emitted (N_{em}) and the number of those absorbed (N_{ab}) by the sample using the relation

$$\Phi_f = N_{em}/N_{ab} = (E_c - E_a)/(L_a - L_c), \qquad (4)$$

where E_c is the integrated luminescence of the sample caused by direct excitation, E_a is the integrated luminescence from an empty integrating sphere (without the sample, only a blank), L_a is the integrated excitation profile from an empty integrating sphere, and L_c is the integrated excitation profile when the sample is directly excited by the incident beam. Under the 400 nm excitation, the quantum efficiency of $Ba_2Ca(BO_3)_2$：$2\% Eu^{2+}$ phosphor were calculated by integrating emission counts from the 450 nm to 700 nm wavelength range. The value is found to be about 72%. Thus, the $Ba_2Ca(BO_3)_2$： $2\% Eu^{2+}$ phosphor demonstrates a high quantum

efficiency.

4　Conclusion
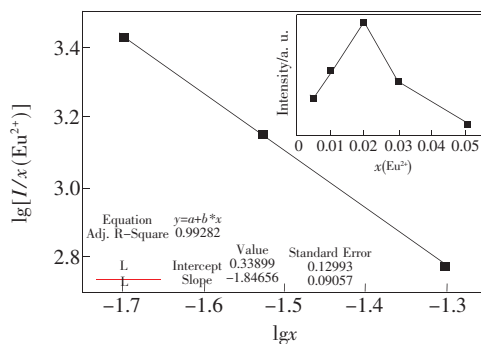
$Ba_2Ca(BO_3)_2$: Eu^{2+} phosphors have been synthesized by the high temperature solid-state method. $Ba_2Ca(BO_3)_2$: Eu^{2+} shows an asymmetrically single green emission band with a maximum at 537 nm, and for 537 nm emission, the excitation spectrum presents a broad absorption from 200 to 500 nm with a peak at 400 nm. The Eu^{2+} doped concentration not only influences the emission intensities of Ba_2Ca-

$(BO_3)_2$: Eu^{2+} but also occurs to the concentration quenching effect. The critical distance can be calculated as 2.64 nm, which agrees well with the value (2.11 nm) deriving from the experimental data. The concentration quenching mechanism of Eu^{2+} in $Ba_2Ca(BO_3)_2$: Eu^{2+} phosphor is determined to be d-d interaction. The CIE chromaticity coordinates of $Ba_2Ca(BO_3)_2$: $x\%Eu^{2+}$ ($x = 0.5, 1, 2, 3, 5, 7$) were slightly varied with increasing the Eu^{2+} concentration, and for $x = 2$, the quantum efficiency is found to be about 72%.

References：

[1] Lin H, Liang H, Zhang G, *et al.* The luminescence of Eu^{3+} activated $Ba_2Mg(BO_3)_2$ phosphors [J]. *Appl. Phys.* A, 2011, 105(1):143-147.

[2] Yuan S, Yang Y, Zhang X, *et al.* Eu^{2+} and Mn^{2+} codoped $Ba_2Mg(BO_3)_2$——new red phosphor for white LEDs [J]. *Opt. Lett.*, 2008, 33(23):2865-2867.

[3] Lin H, Liang H, Tian Z, *et al.* Luminescence of $Ba_2Ca(BO_3)_2$: Ce^{3+}-influence of charge compensator, energy transfer and LED application [J]. *J. Phys.* D：*Appl. Phys.*, 2009, 42(16):165409-1-9.

[4] Xiao F, Xue Y N, Ma Y Y, *et al.* $Ba_2Ca(B_3O_6)_2$: Eu^{2+}, Mn^{2+}：A potential tunable blue-white-red phosphors for white light-emitting diodes [J]. *Physica* B, 2010, 405(3):891-895.

[5] Song E, Zhao W, Zhang W, *et al.* Fluorescence emission spectrum and energy transfer in Eu and Mn co-doped Ba_2Ca-$(BO_3)_2$ phosphors [J]. *J. Lumin.*, 2010, 130:2495-2499.

[6] Hu Y, Yin P, Cheng H, *et al.* Luminescent properties of blue phosphor $Ba_2CaB_6O_{12}$: Eu^{2+} under vacuum-ultraviolet and ultraviolet excitation [J]. *Indian J. Chem.*, 2007, 46A:428-431.

[7] Liang H, Lin H, Zhang G, *et al.* Luminescence of Ce^{3+} and Pr^{3+} doped $Sr_2Mg(BO_3)_2$ under VUV-UV and X-ray excitation [J]. *J. Lumin.*, 2011, 131:194-198.

[8] Wang R, Xu J, Chen C. Fabrication and luminescent properties of $Sr_3B_2O_6$: Eu^{3+}, Na^+ phosphor for white LED applications [J]. *Chin. J. Lumin.* (发光学报), 2011, 32(10):983-987 (in Chinese).

[9] Zhang J S, Liang Z Q, Zhong H Y, *et al.* Enhanced red photoluminescence in Eu^{3+} and Bi^{3+} codoped $LaMgB_5O_{10}$ based on UV/blue LEDs excitation [J]. *Chin. J. Lumin.* (发光学报), 2011, 32(12):1210-1215 (in Chinese).

[10] Zhang X, Fei L, Shi J, *et al.* Eu^{2+}-activated $Ba_2Mg(BO_3)_2$ yellow-emitting phosphors for near ultraviolet-based light-emitting diodes [J]. *Physica* B, 2011, 406(13):2616-2620.

[11] Yao S S, Xue L H, Yan Y W. Concentration quenching of Eu^{2+} in $Ba_2Mg(BO_3)_2$: Eu^{2+} phosphor [J]. *Curr. Appl. Phys.*, 2011, 11(3):639-642.

[12] Verstegen J M P J. The luminescence of Tb^{3+} in borates of the composition $X_2Z(BO_3)_2$ ($X =$ Ba, Sr; $Z =$ Ca, Mg) [J]. *J. Electrochem. Soc.*, 1974, 121(12):1631-1633.

[13] Akella A, Keszler D A. Structure and Eu^{2+} luminescence of dibarium magnesium orthoborate [J]. *Mater. Res. Bull.*, 1995, 30(1):105-111.

[14] Diaz A, Keszler D A. Red, green, and blue Eu^{2+} luminescence in soid-state borates：a structure-property relationship [J]. *Mater. Res. Bull.*, 1996, 31(2):147-151.

[15] Diaz A, Keszler D A. Eu^{2+} luminescence in the borates $X_2Z(BO_3)_2$ ($X =$ Ba, Sr; $Z =$ Ca, Mg) [J]. *Chem. Mater.*, 1997, 9:2071-2077.

[16] Liu L Y, Zhang Y L, Hao J Q, *et al.* Thermoluminescence characteristics of terbium-doped $Ba_2Ca(BO_3)_2$ phosphor [J]. *Phys. Stat. Sol.* (a), 2005, 202(14):2800-2806.

[17] Liu L Y, Zhang Y L, Hao J Q, *et al.* Thermoluminescence studies of rare earth doped $Sr_2Mg(BO_3)_2$ phosphor [J].

Mater. Lett. , 2006, 60(5):639-642.

[18] Lin H, Liang H, Tian Z, *et al*. Vacuum-ultraviolet-vis luminescence of dibarium magnesium orthoborate $Ba_2Mg(BO_3)_2$ doped with Ce^{3+} and Eu^{2+} ions [J]. *J. Mater. Res.* , 2006, 21(4):864-869.

[19] Lin H, Liang H, Han B, *et al*. Luminescence and site occupancy of Ce^{3+} in $Ba_2Ca(BO_3)_2$ [J]. *Phys. Rev.* B, 2007, 76(3):035117-1-8.

[20] Li P L, Wang Z J, Yang Z P, *et al*. Luminescence and site occupancy of Eu^{2+} in $Ba_2Ca(BO_3)_2$ [J]. *Chin. Phys. Lett.* , 2011, 28(1):017801-1-3.

[21] Blasse G. Energy transfer between inequivalent Eu^{2+} ions [J]. *J. Solid State Chem.* , 1986, 62(2):207-211.

[22] Dexter D L, Schulman J H. Theory of concentration quenching in inorganic phosphors [J]. *J. Chem. Phys.* , 1954, 22(6):1063-1070.

[23] van Uitert L G. Characterization of energy transfer interactions between rare earth ions [J]. *J. Electrochem. Soc.* , 1967, 114(10):1048-1053.

[24] Ozawa L, Jaffe P M. The mechanism of the emission color shift with activator concentration In^{3+} activated phosphors [J]. *J. Electrochem. Soc.* , 1971, 118(10):1678-1679.

[25] Xie R J, Hirosaki N, Sakuma K, *et al*. Eu^{2+}-doped Ca-α-SiAlON：A yellow phosphor for white light-emitting diodes [J]. *Appl. Phys. Lett.* , 2004, 84(26):5404-5406.

[26] De Mello J C, Wittmann H F, Friend R H. An improved experimental determination of external photoluminescence quantum efficiency [J]. *Adv. Mater.* , 1997, 9(3):230-232.

[27] Pålsson L O, Monkman A P. Measurements of solid-state photoluminescence quantum yields of films using a fluorimeter [J]. *Adv. Mater.* , 2002, 14(10):757-758.